

Discrete-Time Sliding Mode Control based on Exponential Reaching Law of a Pneumatic Artificial Muscle Actuator

Quy-Thinh Dao*

Hanoi University of Science and Technology, Hanoi, Vietnam
*thinh.daoquy@hust.edu.vn

Trung-Kien Le Tri*

Hanoi University of Science and Technology, Hanoi, Vietnam
*kien.ltt181559@sis.hust.edu.vn

ABSTRACT

In this paper, a discrete-time sliding mode control (DSMC) approach based on exponential reaching law (ERL) is developed for a pneumatic artificial muscle (PAM) system to achieve high tracking performance and chattering alleviation. The proposed controller is designed based on an exponential term that dynamically adapts to the variation of the switching function, thus guarantees finite steps convergence and chattering phenomenon reduction simultaneously. Moreover, the effectiveness of the designed controller and its stability on a dual actuator PAM-driven system is demonstrated under various conditions. In addition, a leg-gait pattern is set as trajectory tracking for further validation. Finally, experiment results show that the proposed approach is effective and promising for rehabilitation applications.

Keywords: *Pneumatic Artificial Muscle; Discrete-time Sliding Mode Control; Exponential Reaching Law; Chattering Phenomenon*

Introduction

In recent years, the rising demand for robotic applications in the human-robot interaction field has gained emerging interests on soft actuators. The key features of these types of actuators are flexibility and inherent compliance, which are the requirement for possible human-friendly robots. PAM is a

lightweight actuator with a cylinder shape, imitates human muscle that generates retraction by pressurized air filling its fiber-covered bladder. Due to many advantages of flexibility, inherently compliant, high power-to-weight ratio, low cost, ease of maintenance, cleanliness, etc. PAM-based systems are mostly used in manipulators [1, 2], rehabilitation robotics [3], medical devices [4], and many others [5, 6]. However, the PAM is known for its strong non-linearity and uncertainty, high hysteresis behavior, hence pose a great challenge in achieving good tracking performance. Therefore, various control strategies have been proposed to overcome these problems in controlling the PAM-driven system. An advanced nonlinear PID-based controller is introduced in [7] for positioning control problems and hysteresis compensation. In [8], the authors implemented an inverse fuzzy model to PID controller to achieve good angle output performance of a PAM robot arm. Cascade position control PID-based controllers using hysteresis model such as modified Prandtl-Ishlinskii model, Maxwell-slip model are designed to compensate the nonlinearity in [9, 10]. These enhanced PID control methods have been widely used yet shown their drawback in the lack of robustness against hysteresis effect and high nonlinearity of PAMs.

It has been acknowledged that sliding mode control (SMC) is an effective robust control strategy for PAMs based systems in the presence of uncertainties and disturbances [11–18]. Nevertheless, with the rapid development of digital controllers, studying the discrete-time sliding mode control (DSMC) design has attracted considerable attention. In discrete-type SMC methodology, the control input is updated at the sampling instant only and remains unchanged during the sampling period. Moreover, numerous works of DSMC have been carried out in the literature on many kinds of systems, including the equivalent control approach [15] and the reaching law-based method [16]. Since the chattering phenomenon is a major problem that degrades tracking accuracy in the application of DSMC, this paper is then concentrated on the reaching-law based control strategy which is considered effective against chattering issues. However, there always exists a trade-off between chattering reduction and reaching time as well as robustness. Hence, a reaching-law-based discrete sliding mode control approach that can alleviate the chattering effect while maintaining fast reaching speed and robustness is needed for a PAM-driven system.

To achieve the above-mentioned requirements, this paper proposes a discrete-time sliding mode controller (DSMC) based on a novel exponential reaching law (ERL) for the PAM-based system. The exponential term was first introduced for continuous reaching law in [19] and had been applied in various publications for chattering alleviation but rarely used on discrete control design [20]. By dynamically adjusting to the sliding function, the proposed controller is augmented with chattering alleviation property while significantly improving reaching speed with satisfactory tracking accuracy.

Since the DSMC-ERL is developed in the discrete-time domain, the proposed control algorithm can thus be effortlessly employed in any digital embedded controller. The main contributions of this paper can be summarized as follows:

- A discrete-time sliding mode controller based on exponential reaching law is designed for a dual PAM system in an antagonistic configuration to elevate control accuracy and attenuate the chattering phenomenon.
- The novel exponential reaching law is redesigned in the discrete-time domain for digital implementation purposes. The stability along with finite steps convergence of the controlled system are briefly analysed.
- Experiment results under various challenging operation conditions together with the load as external disturbance and a leg-gait pattern trajectory demonstrate the effectiveness of the proposed approach in rehabilitation application.

The remaining parts of this work are organized as follows. Section 2 presents experimental platform equipment and a mathematical model of the PAM-driven system. In Section 3, the design procedure of ERL-based DSMC is presented. Experiment results and further investigations are then carried out in Section 4. Finally, conclusions are given in Section 5.

Problem statement

System structure

The controlled PAM-based system is presented in Figure 1. The experimental structure consists of two pneumatic artificial muscles (self-made) connected in an antagonistic configuration as muscles in human limbs, with 23 mm of diameter, 400 mm of nominal length. The internal pressure of PAMs is supplied by two proportional pressure regulator valves (SMC, ITV2030-212SX26), creates tension to rotate the pulley wheel. The deflect angle is then measured by a potentiometer angle sensor (WDD35D8T) with measurement accuracy $\pm 0.01^\circ$. In addition, an embedded controller (National Instrument myRIO-1900) is implemented for the control platform, which can be directly monitored and interfaced through LabVIEW software on a personal computer. Figure 2 demonstrates the schematic structure of the dual PAMs arrangement.

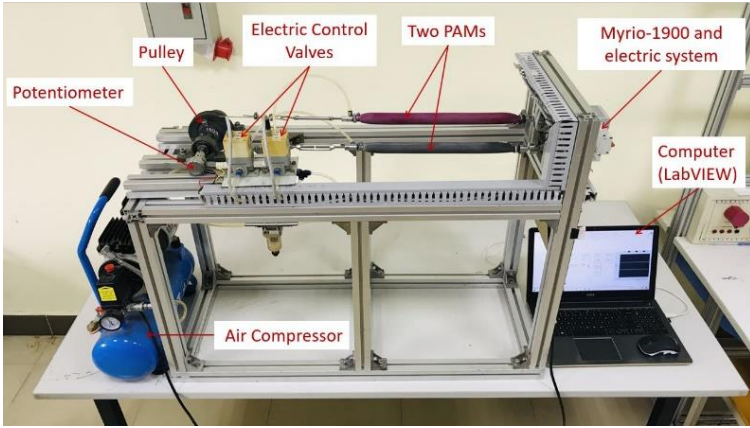


Figure 1: The experiment platform of PAM-based antagonistic configuration.

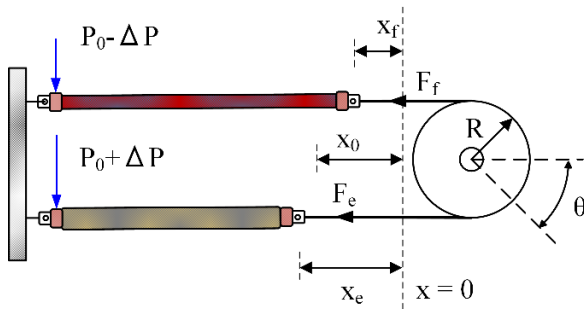


Figure 2: The structure schematic of PAM-based antagonistic configuration.

System model

Considering the PAMs arrangement of control structure illustrated in Figure 2. The dashed line marked by $(x=0)$ represents the position in which two PAMs have complete deflation length. Initially, the pressure P_0 is supplied in both PAMs, they contract to the initial position x_0 . This leads to the initial angle of the pulley $\theta_0 = 0^\circ$. If we increase the pressure on the lower PAM by an amount ΔP and reducing the pressure on the upper one by the same amount, it leads to the difference in their lengths (x_e and x_f). As a result, the joint angle θ of the pulley is created by the following torque:

$$T = (F_e - F_f)R \quad (1)$$

in which F_e and F_f are the forces which are created by each PAM. R is pulley radius.

It can be concluded that the internal pressure input has been simplified to only one variable as the advantage of antagonistic configuration. This can be described as follows:

$$\begin{cases} P_1 = P_0 + \Delta P \\ P_2 = P_0 - \Delta P \end{cases} \quad (2)$$

On the other hand, the control voltages of the electro-pneumatic regulator are designed as:

$$\begin{cases} u_1 = u_0 + u = k_0(P_0 + \Delta P) \\ u_2 = u_0 - u = k_0(P_0 - \Delta P) \end{cases} \quad (3)$$

where u_0 represents the preloaded voltage, k_0 is the proportional coefficient of the internal pressure of PAMs to the valve input voltage, and u is chosen as a manipulated variable. Therefore, the voltage u is the control variable of the closed-loop system that creates contraction on PAMs through air regulation, which deflects the rotational angle θ . Hence, dual pneumatic artificial muscles arranged in antagonistic configuration can be described as a single input single output (SISO) system with the control voltage u of two proportional valves as the input and the output would be the measured joint angle θ . In this case, a SISO discrete-time model is selected to illustrate the PAM-driven system designed above as:

$$y_{k+1} = - \sum_{i=1}^n a_i y_{k-i+1} + \sum_{j=1}^m b_j u_{k-j+1} + p_k \quad (4)$$

where u_k is the control signal of the variable voltage u , y_k is the deflection angle, p_k represents total uncertainties and disturbances, a_i and b_j are model parameters (with $b_j \neq 0$), n and m are the orders of the model such that $n \leq m$. By adopting the parameters estimation approach to construct the system model from input and output data under various scenarios. There are

two input signals including sinusoidal signals and a sine wave with time-varying in both frequency and amplitude are used for the identification purpose.

The mathematical model of PAMs is then identified as a discrete-time second order ARX model, in which $n = m = 2$, achieving a satisfying fit between the estimated and measured data. This whole process is carried out in MATLAB software.

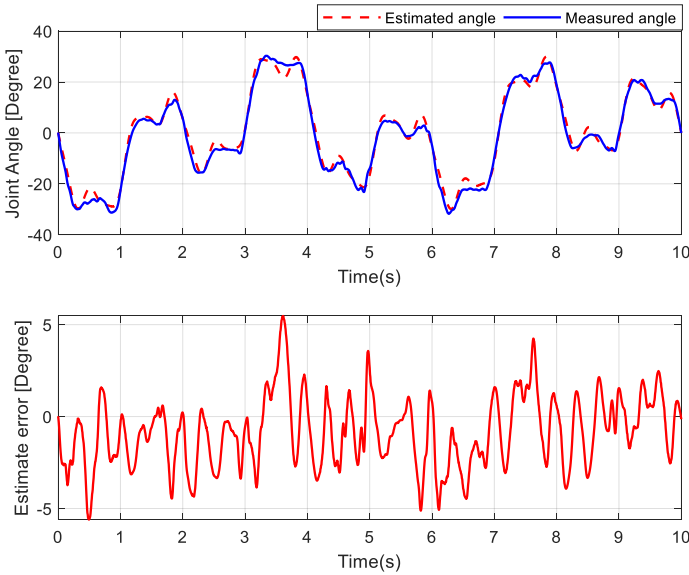


Figure 3: Identification results with the sine wave signal with time-varying amplitude and frequency. The upper sub-figure shows the measured angle (blue line) and its estimated values (dash red line). The lower one is their deviations.

Figure 3 shows the identification results when the second signal is used as the input. The upper sub-figure illustrates the measured angle of the pulley and its estimated values and the lower one is their deviation. It can be seen that the model reaches well approximation with the root mean square error (RMSE) is less than 2.5° and the maximum error does not exceed 5.5° . The specific values of the model parameters are listed in Table 1.

Table 1: Model parameters

Parameters	Values
a_1	-1.9567 ± 0.0092
a_2	-0.9576 ± 0.0128
b_1	0.0126 ± 0.0013
b_2	0.0124 ± 0.0049

Design of the control strategy

In this work, an exponential reaching law is implemented in discrete-time sliding mode control for the PAM-driven system. The proposed reaching law enhances tracking performance with its novel properties of chattering reduction and fast reaching speed without affecting tracking precision. Figure 4 demonstrated the schematic diagram of the proposed control method.

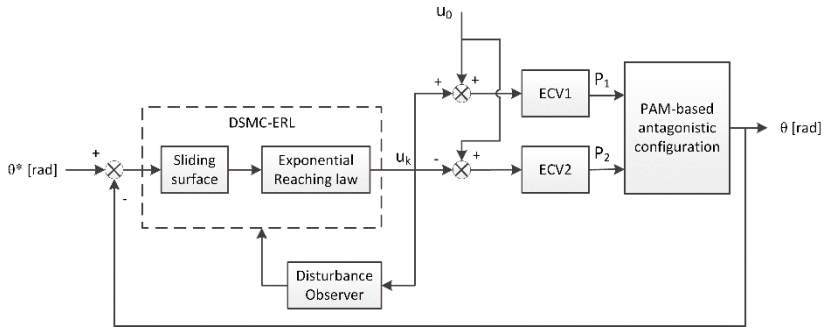


Figure 4: Block diagram of the system controller.

Sliding surface design

Let the tracking error be defined as $e_k = y_k^* - y_k$ with the reference trajectory y_k^* . Considering the following sliding surface:

$$s_k = e_k + \lambda e_{k-1} \quad (5)$$

where λ is a positive constant. Taking the increment of (5), one obtains:

$$s_{k+1} = e_{k+1} + \lambda e_k \quad (6)$$

Based on the discrete-time SISO model selected for the PAMs-driven system in (4), the one-step-forward tracking error can be expressed as follows:

$$e_{k+1} = y_{k+1}^* - y_{k+1} = y_{k+1}^* + \sum_{i=1}^n a_i y_{k-i+1} - \sum_{j=1}^m b_j u_{k-j+1} - p_k \quad (7)$$

where y_{k+1}^* is the one-step-ahead of the reference trajectory. As in control practice, the desired trajectory is predetermined so y_{k+1}^* is assumed to be known. Substituting the tracking error in (7) into (6) gives:

$$s_{k+1} = y_{k+1}^* + \sum_{i=1}^n a_i y_{k-i+1} - \sum_{j=1}^m b_j u_{k-j+1} - p_k + \lambda(y_k^* - y_k) \quad (8)$$

Assumption 1 *The generalized disturbance p_k is bounded and slow time-varying as the sampling time $T_s = 5ms$ is rather small. Therefore, p_k is proved to possess a lemma as follows [21].*

Lemma 1 $p_k = O(T_s)$, $p_k - p_{k-1} = O(T_s^2)$, and $p_k - 2p_{k-1} + p_{k-2} = O(T_s^3)$, where $O(T_s)$ is the error boundary with thickness.

Owing to the reason that the disturbance p_k is intricate to measure in general practice, thus letting the disturbance p_k be simply estimated by its decrement value as:

$$\hat{p}_k = p_{k-1} = y_k + \sum_{i=1}^n a_i y_{k-i} - \sum_{j=1}^m b_j u_{k-j} \quad (9)$$

where \hat{p}_k is the estimation of disturbance p_k . Hence, the disturbance estimation error $\tilde{p}_k = p_k - \hat{p}_k$ can be given as follows:

$$\tilde{p}_k = p_k - p_{k-1} = O(T_s^2) \quad (10)$$

By substituting (9) into the expression of the sliding function in (8), it yields:

$$s_{k+1} = y_{k+1}^* + \sum_{i=1}^n a_i y_{k-i+1} - \sum_{j=1}^m b_j u_{k-j+1} - \hat{p}_k - \tilde{p}_k + \lambda(y_k^* - y_k) \quad (11)$$

Discrete-time exponential reaching law

In pursuance of achieving chattering alleviation, finite convergence steps, and robustness simultaneously, the discrete reaching law proposed in this work is given by:

$$s_{k+1} = s_k - \frac{\gamma}{\psi(k)} \text{sign}(s_k), \quad g > 0 \quad (12)$$

where,

$$\psi(k) = \delta_0 + (1 - \delta_0)e^{-\alpha|s_k|^p} \quad (13)$$

in which d_0 , a are strictly positive constants, and d_0 is less than one, p is a strictly positive integer. It can be concluded that the ERL component $\gamma(k)$ is always strictly positive and does not affect the stability of the system. This exponential term allows the controller to dynamically adapt to the variations of the switching function by letting the gain vary between g and g/d_0 , thus reducing the chattering phenomenon. For this advantage, the proposed controller is greatly enhanced by the property of chattering reduction as well as having the ability to improve the reaching speed compared to the conventional one.

Remark 1 If d_0 are chosen to be equal to one, the designed controller becomes the DSMC with the constant rate reaching law. In other words, the conventional reaching law is a particular case of the proposed approach.

Then the proposed control signal is found from the reaching law by substituting sliding variable s_{k+1} from (12) into (7) and further solving for u_k which leads to:

$$u_k = (b_1)^{-1} \left[y_{k+1}^* + \sum_{i=1}^n a_i y_{k-i+1} - \sum_{j=2}^m b_j u_{k-j+1} - \hat{p}_k - \tilde{p}_k + \lambda(y_k^* - y_k) - s_k + \frac{\gamma}{\psi(k)} \text{sign}(s_k) \right] \quad (14)$$

According to (10), the disturbance estimation error $\hat{\delta}_k$ is bounded and rather small in practice applications that is negligible. Hence, the viable final form of the control signal u_k in the absence of $\hat{\delta}_k$ can be rewritten as

$$u_k = (b_1)^{-1} \left[y_{k+1}^* + \sum_{i=1}^n a_i y_{k-i+1} - \sum_{j=2}^m b_j u_{k-j+1} - \hat{p}_k + \lambda(y_k^* - y_k) - s_k + \frac{\gamma}{\psi(k)} \text{sign}(s_k) \right] \quad (15)$$

Stability analysis

As Sarpturk et al. [22] pointed out that the control for discrete-time systems must have upper and lower bounds depending on the sampling instant and uncertainties. This gives the following sliding-and-convergence condition:

$$|s_i(k+1)| < |s_i(k)| \quad (16)$$

Following the reaching law (12), if $s_k < 0$ it can be derived that:

$$s_{k+1} - s_k = \frac{\gamma}{\psi(k)} > 0 \quad (17)$$

Likewise, if $s_k > 0$, equation (12) yields:

$$s_{k+1} - s_k = -\frac{\gamma}{\psi(k)} < 0 \quad (18)$$

From (17) and (18), we obtain:

$$|s(k+1)| < |s(k)| \quad (19)$$

Hence, the exponential reaching law satisfies the aforementioned condition which ensures the stability and finite steps convergence of the proposed controller.

Experimental results

In this section, to verify the effectiveness of the proposed control approach, the dual PAM system is carried through a series of experiments with different reference trajectories. These include a leg-gait pattern employed as the desired trajectory to investigate the applicability of the proposed control method in the rehabilitation robot field. The established experimental configuration has been introduced in section 2 as presented in Figure. 1. The sampling constant T_s of the controller is set to be 5 ms. The control algorithm is first implemented on a personal computer by using LabVIEW software before being downloaded to NI MyRIO-1900 embedded controller. The proposed control approach is also compared with a conventional discrete-time sliding mode controller (DSMC) in terms of tracking performances under the same operating conditions. Model parameters of the PAMs-driven system are shown in Table 1. The control parameters of the proposed DSMC-ERL are fine-tuned by trial and listed in Table 2.

Table 2: Parameters of the DSMC ERL-based controller

Parameters	λ	γ	δ_0	α	p
Values	1	0.5	0.2	0.05	1

Tracking sinusoidal trajectories

In this following part, sinusoidal signals with an amplitude of 20° and frequencies ranging from 0.2 Hz to 1.0 Hz are chosen as the reference trajectories. Representative comparison results of the DSMC and proposed controller ERL are shown in Figure. 4. It can be observed that the conventional DSMC controller leads to a serious chattering phenomenon, and also gives the worse performance with an unacceptable range of tracking error at about $\pm 5.0^\circ$. The chattering behavior is weakened by the exponential term in the ERL controller so that its tracking performance can achieve good precision with less than 3.0° of tracking error in steady-state. The ERL controller has much fewer control chatters as the advantage of exponential term, it also achieves a better smooth control with almost chattering free operation and good handle the overshoot problem in transient state.

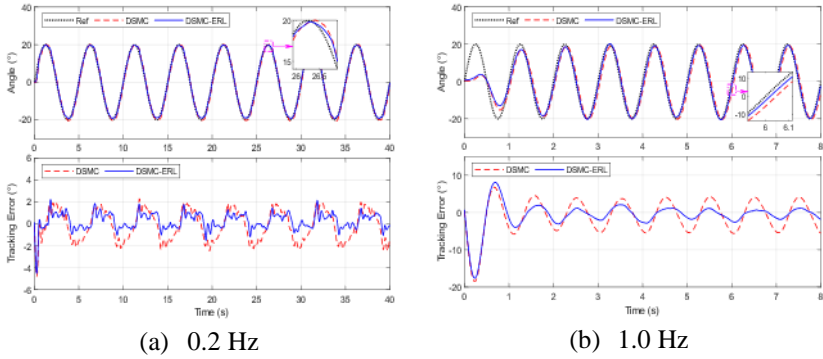


Figure 4: Experiment results for tracking sinusoidal trajectory without a load.

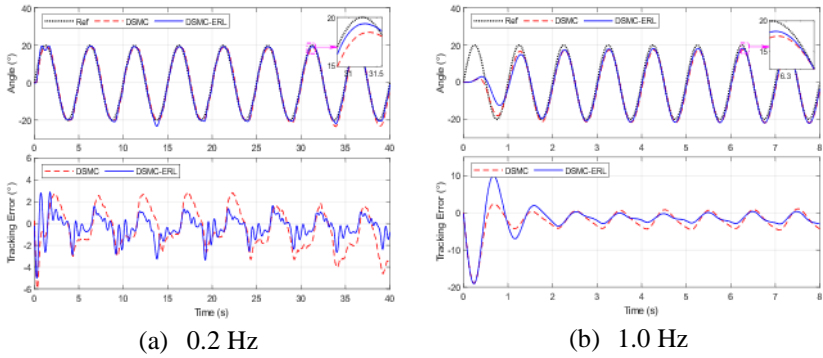


Figure 5: Experiment results for tracking sinusoidal trajectories and driving a load $m = 5\text{kg}$.

To further investigate the effectiveness of the proposed control algorithm, a load $m = 5\text{ kg}$ is added to the system. The tracking performance results along with tracking errors and control signals are typified in Figure 5. It can be found that the DSMC and the ERL are stable and robust with load resulted in not too much upraising of the tracking error. Besides, the designed controller provides good chattering alleviation in the control signal as well as fast response speed. Therefore, the better performance of the proposed ERL is verified by the experimental results. To give a quantitative analysis, the root mean square errors (RMSE) of both controllers are provided in Table 3.

Table 3: RMSE ($^{\circ}$) of comparative controllers with regard to sinusoidal tracking experiment

Frequency	No load		m = 5kg	
	DSMC	ERL	DSMC	ERL
0.2Hz	1.62	1.28	1.92	1.82
0.5Hz	2.21	1.66	2.79	2.13
0.8Hz	2.70	3.13	3.87	3.59
1.0Hz	4.21	3.73	4.62	4.18

Tracking the human-gait pattern trajectories

As an extension to examine the applicability of the designed controller in rehabilitation robotic, a leg-gait pattern, which is employed and modified from the knee gait data in DA. Winter's textbook [24], is set to be the desired trajectory. The frequency of the desired trajectory is ranged from 0.1 to 0.5 Hz. The 0.5 Hz trajectory is equivalent to about 2.5 km/h of the walking speed. The illustrative tracking results are shown in Figure 6. It can be seen that the chattering phenomenon still somewhat occurs at the direction changing point in the figure for 0.5 Hz of DSMC, especially in the low amplitude part of the signal. On the other hand, the figure for DSMC-ERL shows almost no chatter over the tracking course, which comes from the benefit of the ERL reaching law. Furthermore, in the case of 0.5Hz frequency, the tracking performance of the conventional DSMC is strongly affected by the hysteresis problem and slow response behavior of the PAMs, which lead to a huge RMSE different gap between the two controllers. With less than 5.0° maximum error in steady-state, the DSMC-ERL once again shows great performance, decent tracking accuracy with chattering-free control advantage even for tracking a fairly difficult trajectory as knee movement.

A similar load $m = 5$ kg is also added to the system as an external disturbance. Figure 7 illustrates the two particular tracking results comparing the DSMC-ERL controller and its counterparts. It is observed that the DSMC controller performs even worse tracking accuracy in the case of a 5kg load. The maximum steady-state error is rather high up to 9.0° . Meanwhile, the ERL-based DSMC can give a better control performance under loading conditions with the maximum steady-state error is less than 3.0° in all scenarios. As expected, the ERL-based controller also shows no sign of chattering behavior which comes from the adaption of the control gain under disturbance. The quantitative comparisons of the two controllers in terms of RMSEs are detailed in Table 4.

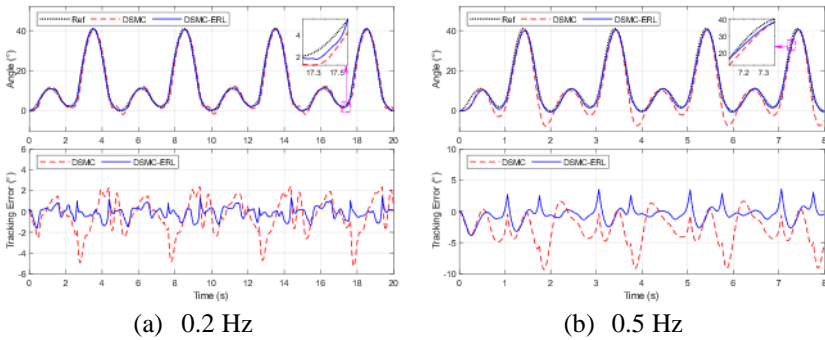


Figure 6: Experiment results for tracking knee movement trajectory without a load.

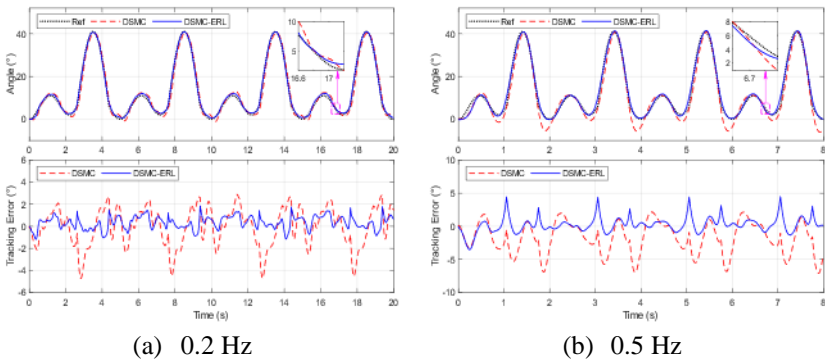


Figure 7: Experiment results for tracking knee movement trajectory and driving a load $m = 5$ kg.

Table 4: RMSE ($^{\circ}$) of comparative controllers with regard to the knee gait pattern tracking experiment

Frequency	No load		m = 5 kg	
	DSMC	ERL	DSMC	ERL
0.1 Hz	0.83	0.43	0.97	0.46
0.2 Hz	1.73	1.47	2.75	2.03
0.5 Hz	3.0	2.16	3.67	2.89

Conclusion and Discussion

In this paper, a discrete-time sliding mode controller based on exponential reaching law has been proposed for a mechanism of PAMs in the antagonistic configuration. The exponential reaching law is introduced to attenuate the chattering and enhance the tracking performance of DSMC in both transient and steady-state. The tracking accuracy of the ERL-based controller has been analyzed and the effectiveness of the proposed reaching law has been verified through various scenarios. Finally, experiment results clearly show the validity of the designed controller in dealing with the chattering phenomenon and achieving satisfactory tracking performance. In comparison to the recent researches about trajectory tracking control of PAM, the proposed ERL-based controller achieves a comparative performance in both cases with and without a load. For example, when tracking a 0.5 Hz gait pattern with 40° amplitude without a load, the RMSEs of the ERL-based controller reaches 2.16° (5.4% of amplitude). Meanwhile, the fractional order-based controller in [15] achieves an accuracy of 4.5% with the frequency of the desired trajectory is 0.4Hz equivalent to 2.5 seconds of gait cycle time. When a load is added to the system as an external disturbance, the control performance degrades with the maximum tracking error is about 5.0° but it still accords with the accuracy of LOKOMAT [23], a well known commercial gait training system that has a maximum tracking error is 15° with a participant.

In summary, an enhanced SMC controller is proposed in this paper. The “chattering” phenomenon is reduced by implementing the exponential reaching law. The good performance when tracking a human gait pattern demonstrates the promising applicability of the proposed controller in assistive robot systems.

Acknowledgment

This research is funded by Hanoi University of Science and Technology (HUST) under project number T2020-TT-002.

References

- [1] L. Zhao, X. Liu, t. Wang, “Trajectory tracking control for double-joint manipulator systems driven by pneumatic artificial muscles based on a nonlinear extended state observer”. *Mechanical Systems and Signal Processing*, vol. 122, pp. 307-320, 2019.
- [2] M. A. Mat Dzahir and S. Yamamoto, “Dynamic Modeling of McKibben

- Muscle Using Empirical Model and Particle Swarm Optimization Method”. *Applied Sciences*, vol. 9, no. 12, pp. 2538, 2019.
- [3] Zhang, C.; Hu, J.; Ai, Q.; Meng, W.; Liu, Q. “Impedance control of a pneumatic muscles-driven ankle rehabilitation robot” *Intell. Robot. Appl.*, vol. 10462, pp. 301-312, 2017.
- [4] S. K. Banala, Deok Hun Kim, S. K. Agrawal, and J. P. Scholz, “Robot Assisted Gait Training with Active Leg Exoskeleton (ALEX)”. *IEEE Transactions on Neural Systems and Rehabilitation Engineering*, vol. 17, no. 1, pp. 2-8, 2009.
- [5] Q.-T. Dao and S. Yamamoto, “Assist-as-Needed Control of a Robotic Orthosis Actuated by Pneumatic Artificial Muscle for Gait Rehabilitation”. *Applied Science*, vol. 8, no. 4, pp. 449, 2018.
- [6] S. Hussain, S. Q. Xie, and P. K. Jamwal, “Control of a robotic orthosis for gait rehabilitation”. *Robotic and Autonomous Systems*, vol. 61, no.9. pp. 911-919, 2013.
- [7] G. Andrikopoulos, G. Nikolakopoulos, and S. Manesis, “Advanced Nonlinear PID-Based Antagonistic Control for Pneumatic Muscle Actuators”. *IEEE Transaction on. Industrial Electronics*, vol. 61, no. 12, pp. 6926–6937, 2014.
- [8] H. P. H Anh and K. K. Ahn, “Hybrid control of a pneumatic artificial muscle (PAM) robot arm using an inverse NARX fuzzy model,” *Engineering Applications of Artificial Intelligence*, vol. 24, no. 4, pp. 697-716, 2011.
- [9] S. Xie, J. Mei, H. Liu, and Y. Wang, “Hysteresis modeling and trajectory tracking control of the pneumatic muscle actuator using modified Prandtl-Ishlinskii model,” *Mechanism and Machine Theory*, vol. 120, pp. 213-224, 2018
- [10] T. Vo-Minh, T. Tjahjowidodo, H. Ramon, and H. V. Brussel, “A New Approach to Modeling Hysteresis in a Pneumatic Artificial Muscle Using The Maxwell-slip Model”. *IEEE/ASME Transactions on Mechatronics*, vol. 16, no. 1, pp. 177-186, 2011.
- [11] J. H. Lilly and P. M. Quesada, “A two-input sliding-mode controller for a planar arm actuated by four pneumatic muscle groups,” *IEEE Transactions on Neural Systems and Rehabilitation Engineering*, vol. 12, no. 3, pp. 349-359, 2004.
- [12] K. Xing, J. Huang, Y. Wang, J. Wu, Q. Xu, and J. He, “Tracking control of pneumatic artificial muscle actuators based on sliding mode and non-linear disturbance observer”. *IET Control Theory & Application*, vol. 4, no. 10, pp. 2058-2070, 2010.
- [13] C.-J. Chiang and Y.-C. Chen, “Neural network fuzzy sliding mode control of pneumatic muscle actuators,” *Engineering Applications of Artificial Intelligence*, vol. 65, pp. 68-86, 2017.
- [14] C. P. Vo, X. D. To, and K. K Ahn, “A Novel Adaptive Gain Integral

- Terminal Sliding Mode Control Scheme of a Pneumatic Artificial Muscle System With Time-delay Estimation”. *IEEE Access*, vol. 7, pp. 141133-141143, 2019.
- [15] Q.-T. Dao, M.-L. Nguyen, S. Yamamoto, “Discrete-Time Fractional Order Integral Sliding Mode Control of an Antagonistic Actuator Driven by Pneumatic Artificial Muscles” *Applied Sciences*, vol. 9, no. 12, pp. 2503, 2019.
- [16] Fellag, R.; Hamerlain, M.; Laghrouche, S; Achour, N. “Adaptive discrete sliding mode control of a pneumatic artificial muscle robot”. *5th Int. Conf. on Electrical Engineering. (ICEE) 2017*.
- [17] L. Zhao, Q. Li, B. Liu, and H. Cheng, “Trajectory Tracking Control of a One Degree of Freedom Manipulator Based on a Switched Sliding Mode Controller with a Novel Extended State Observer Framework,” *IEEE Transactions on Systems, Man, and Cybernetics: Systems*, vol. 49, no. 6, pp. 1110-1118, 2019.
- [18] L. Melkou and M. Hamerlain, "High Order Homogeneous Sliding Mode Control for a Robot Arm with Pneumatic Artificial Muscles," *IECON 2019-45th Annual Conference of the IEEE Industrial Electronics Society*, 2019.
- [19] C. J. Fallaha, M. Saad, H. Y. Kanaan and K. Al-Haddad, “Sliding-Mode Robot Control With Exponential Reaching Law,” *IEEE Transactions on Industrial Electronics*, vol. 58, no. 2, pp. 600-610, 2011.
- [20] K. B. D and S. Thomas, “Power rate exponential reaching law for enhanced performance of sliding mode control,” *International Journal of Control, Automation Systems*, vol. 15, no. 6, pp. 2636-2645, 2017.
- [21] K. Abidi, J.-X Xu, and Y. Xinghuo, “On the Discrete-Time Integral Sliding-Mode Control,” *IEEE Transactions on Automatic Control*, vol. 52, no. 4, pp. 709-715, 2017.
- [22] S. Z. Sarpturk, Y. Istefanopulos, and O. Kaynak, “On the stability of discrete-time sliding mode control systems,” *IEEE Transactions on Automatic Control*, vol. 32, no. 10, pp. 930-932, 1987.
- [23] R. Riener, L. Lunenburger, S. Jezernik, M. Anderschitz, G. Colombo, and V. Dietz, “Patient-Cooperative Strategies for Robot-Aided Treadmill Training: First Experimental Results,” *IEEE Transactions on Neural Systems and Rehabilitation Engineering*, vol. 13, no. 3, pp. 380–394, 2005.
- [24] Winter, D.A. “*Biomechanics and Motor Control of Human Movement*”, 3rd ed.; University of Waterloo Press: Waterloo, ON, Canada, 1990.